PERFORMANCE ANALYSIS OF A HARDWARE IMPLEMENTED COMPLEX SIGNAL KURTOSIS RADIO-FREQUENCY INTERFERENCE DETECTOR

Adam J. Schoenwald [1]
Damon C. Bradley [1], Priscilla N. Mohammed [1,2], Jeffrey R. Piepmeier [1], Mark Wong [1]

(1) NASA Goddard Space Flight Center, Greenbelt, MD
(2) Goddard Earth Sciences Technology and Research, Morgan State University

ABSTRACT

In the field of microwave radiometry, Radio Frequency Interference (RFI) consistently degrades the value of scientific results. Through the use of digital receivers and signal processing, the effects of RFI on scientific measurements can be reduced depending on certain circumstances. As technology allows us to implement wider band digital receivers for radiometry, the problem of RFI mitigation changes. Our work focuses on finding a detector that outperforms real kurtosis in wide band scenarios. The algorithm implemented is a complex signal kurtosis detector which was modeled and simulated. The performance of both complex and real signal kurtosis is evaluated for continuous wave, pulsed continuous wave, and wide band quadrature phase shift keying (QPSK) modulations. The use of complex signal kurtosis increased the detectability of interference.

Index Terms— Interference, Circularity, Complex Random Process, Radiometer, Digital Receiver, Kurtosis, Complex Kurtosis

1. INTRODUCTION

Radio-frequency interference (RFI) is a known problem for passive remote sensing as evidenced in the L-band radiometers SMOS, Aquarius and more recently, SMAP [1]. Various algorithms have been developed and implemented on SMAP to improve science measurements. This was achieved by the use of a digital microwave radiometer [1]. RFI mitigation becomes more challenging for microwave radiometers operating at higher frequencies in shared allocations. At higher frequencies larger bandwidths are also desirable for lower measurement noise further adding to processing challenges. This work focuses on finding improved RFI mitigation techniques that will be effective at additional frequencies and at higher bandwidths.

To aid the development and testing of applicable detection and mitigation techniques, a wide band RFI algorithm testing environment has been developed using the Reconfigurable Open Architecture Computing Hardware System (ROACH) built by the Collaboration for Astronomy Signal Processing and Electronics Research (CASPER) Group. The testing environment also consists of various test equipment used to reproduce typical signals that a radiometer may see including those with and without RFI. The testing environment permits quick evaluations of RFI mitigation algorithms as well as show that they are implementable in hardware[2].

The algorithm implemented is a complex signal kurtosis detector which was modeled and simulated. The complex signal kurtosis detector showed improved performance over the real kurtosis detector under certain conditions [2]. The real kurtosis is implemented on a SMAP like architecture at 24 MHz bandwidth using the ROACH. Then the real and complex signal kurtosis [3] algorithms were implemented in hardware at 200 MHz bandwidth using the ROACH. In this work, performance of the complex signal kurtosis and the real signal kurtosis are compared. Performance evaluations and comparisons in both simulation as well as experimental hardware implementations were done with the use of receiver operating characteristic (ROC) curves. The complex kurtosis algorithm has the potential to reduce data rate due to onboard processing in addition to improving RFI detection performance.

2. ALGORITHM DESCRIPTION

2.1. Real Signal Kurtosis

Given a complex baseband signal $z(n) = I(n) + jQ(n)$, the fourth standardized moment is computed independently for both the real and imaginary vectors, I and Q as was used in SMAP[3].

$$RSK_I = \frac{\mathbb{E}\left[(I - \mathbb{E}[I])^4\right]}{\mathbb{E}\left[(I - \mathbb{E}[I])^2\right]} - 3 \tag{1}$$

$$RSK_Q = \frac{\mathbb{E}\left[(Q - \mathbb{E}[Q])^4\right]}{\mathbb{E}\left[(Q - \mathbb{E}[Q])^2\right]} - 3 \tag{2}$$

The test statistic, RSK (Real Signal Kurtosis), is then defined as

$$RSK = \frac{|RSK_I| + |RSK_Q|}{2} \tag{3}$$

Thanks to NASA Earth Science Technology Office NNH13ZDA001N ACT Funding

2.2. Complex Signal Kurtosis

Given a complex baseband signal $z(n) = I(n) + jQ(n)$, moments $\alpha_{\ell,m}$ are defined as

$$\alpha_{\ell,m} = \mathbb{E}\left[(z - \mathbb{E}[z])^{\ell}(z - \mathbb{E}[z])^{*m}\right], \quad \ell, m \in \mathbb{Z}_{\geq 0} \tag{4}$$

With $\sigma^2 = \alpha_{1,1}$, Standardized moments $\varrho_{\ell,m}$ can be found as

$$\varrho_{\ell,m} = \frac{\alpha_{\ell,m}}{\sigma^{\ell+m}}, \tag{5}$$

leading to the CSK (Complex Signal Kurtosis) RFI Test statistic used [1,2]

$$C_K = \frac{\varrho_{2,2} - 2 - |\varrho_{2,2}|^2}{1 + \frac{1}{2}|\varrho_{2,2}|^2} \tag{6}$$

2.3. Moment Calculation

The hardware implementation of test statistics uses a moment expansion to perform the computation of higher order statistics. The nomenclature used for raw moments, given the real (I) and imaginary (Q) parts of a complex signal of the r^{th} power is defined as

$$mI^r = \mathbb{E}\left[I^r\right] \tag{7}$$

$$mQ^r = \mathbb{E}\left[Q^r\right] \tag{8}$$

The following full band moments are produced to compute real signal kurtosis.

$$mI^r, mQ^r, r \in \{1, 2, 3, 4\} \tag{9}$$

Additionally the following cross complex moments are generated to compute complex kurtosis.

$$mIQ, mIQQ, mIIQ, mIIQQ \tag{10}$$

In the case of sub-banding, all 12 moments for each polarization are produced for every sub-band.

3. ALGORITHM EVALUATION METHODOLOGY

Evaluation of the complex kurtosis detector was done by forming a binary hypothesis problem. A set of Monte-Carlo simulations were performed under null and active hypotheses. Under the null hypthothesis, our system was injected with band limited white Gaussian noise to simulate a geophysical black body radiation Gaussian process. Under the active hypothesis, interference was added to the Gaussian noise. To determine the detectability of various types of interference, different modulations were used. The modulations tested include narrow band continuous wave (CW) interference, narrow band pulsed continuous wave (PCW) interference, and wide band filtered quadrature phase shift keying (QPSK) modulation. For each type of interference tested, the interference to noise ratio (INR) was varied. The set of simulations performed for each modulation type can be thought of as an INR sweep.

In addition to software simulations, the Monte-Carlo hypothesis testing algorithm evaluation methodology was also implemented in hardware [2] using the CASPER ROACH system. The detection algorithms were implemented on a field programmable gate array (FPGA), and an arbitrary Waveform Generator(AWG) was used to provide the analog to digital converter (ADC) with the test signals. The same Gaussian and Interference models were used for both simulation and hardware verification, although the sample rate differed due to use of oversampling on the AWG to increase the test signal fidelity.

For every combination of modulation and interference to noise ratio, a receiver operating characteristic (ROC) curve was computed through the use of Mote-Carlo simulations. As a figure of merit, the area under the curve (AUC) is calculated for each ROC curve. To even further compress the measurement set into a figures of merit for a particular type of modulation, the INR at which an AUC is 0.75 is interpolated from its surrounding test points. This gives a simple figure of merit to compare detection methods across various modulations.

A block diagram of the algorithm performance methodology and test set-up can be found in Figure 1.

4. ALGORITHM PERFORMANCE RESULTS

The number of samples used to calculate performance changes the detector performance due to statistical convergence, so it is important that is fixed across multiple simulations if the results are to be compared. The number of samples for each Monte-Carlo run, N, is 20000. A cross section of simulated CW RFI results can be seen in Figure 2 in the form of ROC curves at various INRs. As seen in the Figure 2, both RSK and CSK are displayed at an INR of -4, -8, and -9. A gain in performance between real and complex signal kurtosis can be seen by the increase in AUC.

To compare a more thorough set of modulation types, (CW, PCW, and QPSK) , an INR vs AUC plot is provided in Figure 3 and Figure 4. The legend is sorted from most to least detectable interference types. To compare the simulation results with hardware results, the same set of experiments were performed on the hardware implementation aside from PCW modulation. PCW modulation was excluded from hardware simulation to simplify the experimental setup and expedite results.

The hardware results show the same trends in detectability however the overall detection performance is degraded from simulation to hardware. There are a number of possible reasons for reduced performance but this has not been thoroughly analyzed. The performance difference is most likely related to fixed point effects in both the signal generation and acquisition phases. Additionally, the hardware fixed point implemen-

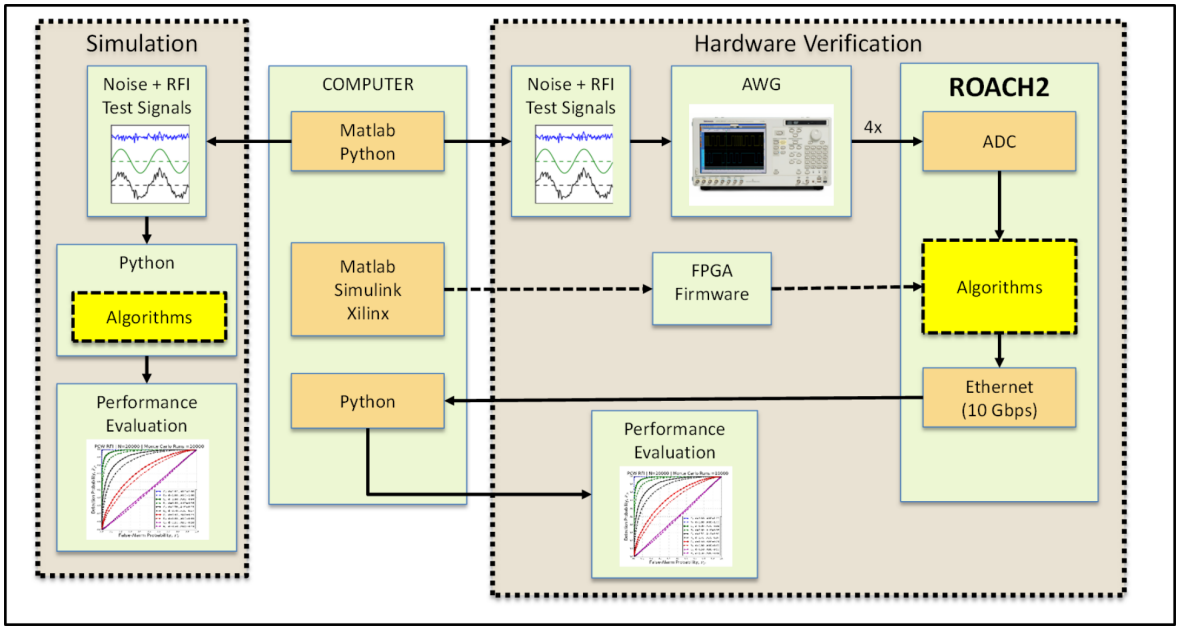

Fig. 1. Block diagram of algorithm performance analysis methodology

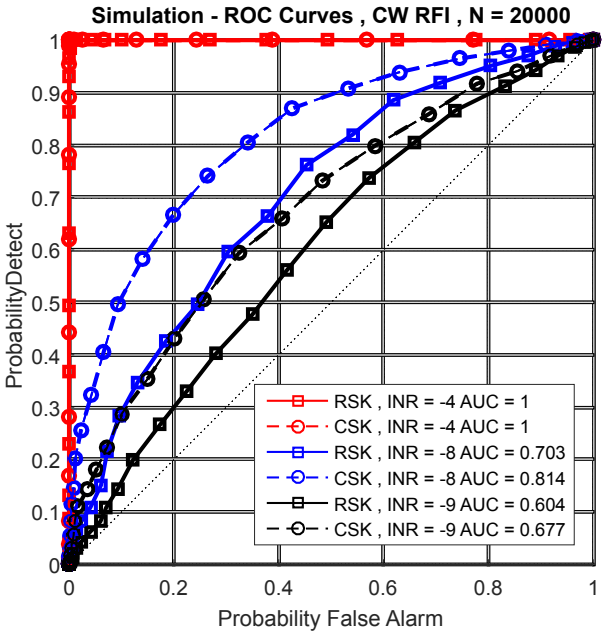

Fig. 2. ROC Curve for narrow band continuous wave modulation. Results from simulation. Sub-banding outperforms full band detector.

tation was not carefully optimized. Performance can likely be increased through careful tuning of fixed point rounding and attenuation stages that were originally introduced to prevent output saturation.

It was previously shown that narrow band interference detectability is improved through the use of channelization before using a kurtosis normality test [4]. Here it is demonstrated that the use of channelization decreases detectability of wide band interference in Figure 5 , as opposed to the gain in the detectability of narrow band interference as seen in Figure 6 . Note that the interference to noise ratios used for these images was selected to show the impact of channelization, and do not match between narrow and wide band modulations.

5. CONCLUSIONS

These results show that the performance of a kurtosis detector will vary depending on the type of modulation being detected. Generally speaking, the real and complex signal kurtosis detectors perform best under pulsed continous wave interference. Additionally, it is seen in both software simulation and hardware implementation that the complex signal kurtosis provides an increase in detectability. In our simulations the use of CSK results in a detectable signal at an INR of 2dB less than RSK in the best case scenario, but performance increase varies across modulation parameters. The increase of computational intensity can be summarized by the hardware necessary to extend the calculation from 8 to 12 moments. Further study would be required to determine if this tradeoff is justifiable depending on end application.

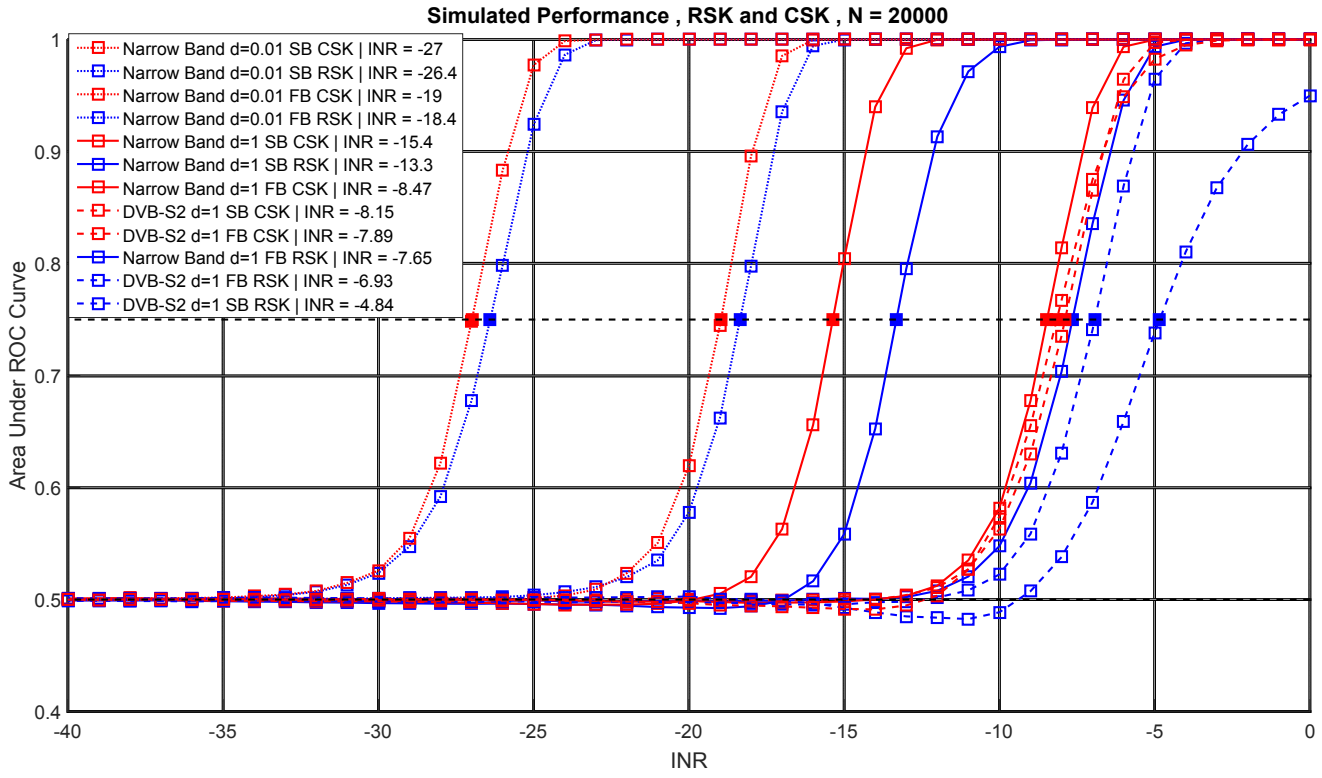

Fig. 3. Simulation results - AUC vs INR. The AUC = 0.75 point was interpolated between test points. Modulations tested include narrow band continuous wave (CW), narrow band pulsed continous wave (PCW) with duty cycle = 1%, and wide band QPSK. PCW is excluded from hardware results.

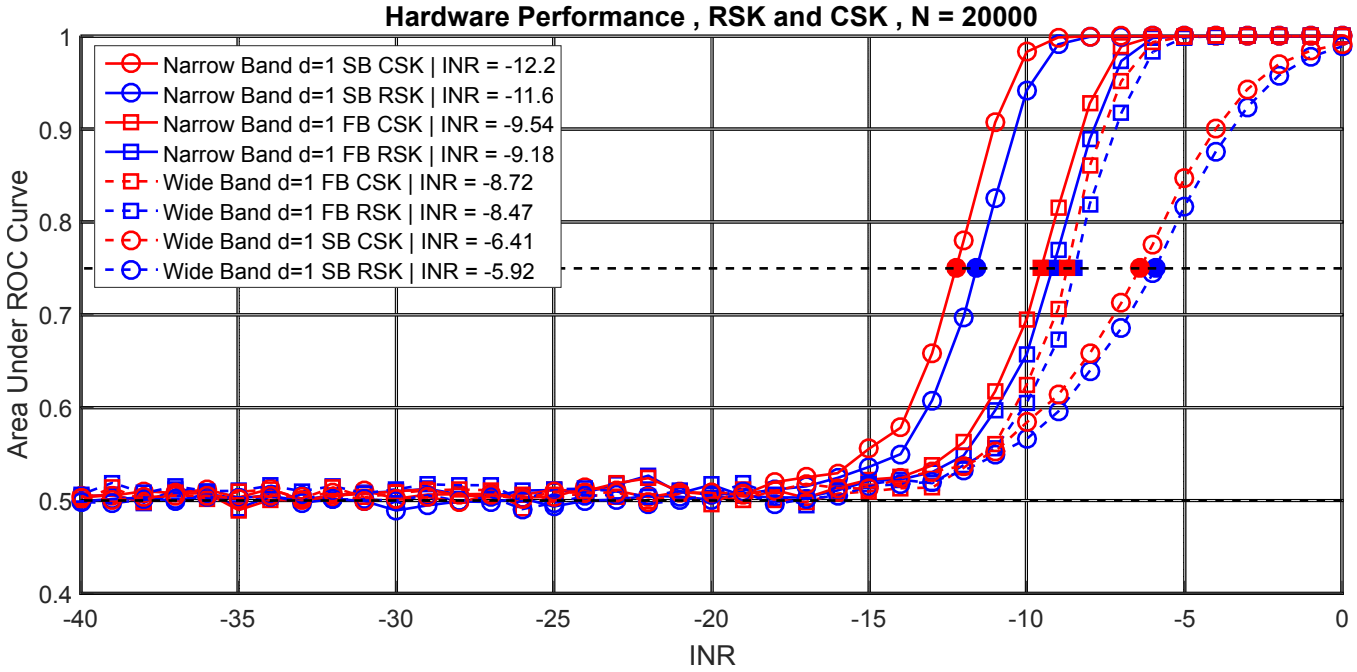

Fig. 4. Hardware results - AUC vs INR. The AUC = 0.75 point was interpolated between test points. Modulations tested include narrow band continuous wave and wide band QPSK only. PCW is excluded from hardware results.

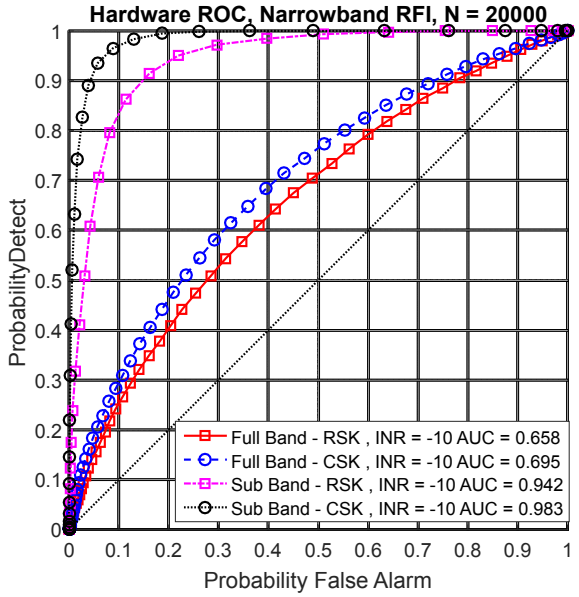

Fig. 5. ROC Curve for narrow band continuous wave modulation. Results from hardware implementation. Sub-banding outperforms full band detector.

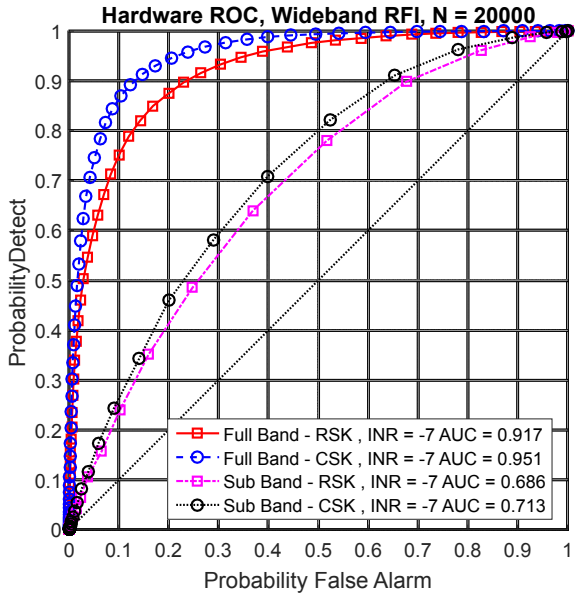

Fig. 6. ROC Curve for wide band QPSK modulation. Results from hardware implementation. Full band detector outperforms sub-banding.

6. REFERENCES

[1] J. R. Piepmeier, J. T. Johnson, P. N. Mohammed, D. Bradley, C. Ruf, M. Aksoy, R. Garcia, D. Hudson, L. Miles, and M. Wong, "Radio-frequency interference mitigation for the soil moisture active passive microwave radiometer," *IEEE Transactions on Geoscience and Remote Sensing*, vol. 52, no. 1, pp. 761–775, Jan 2014.

[2] D. C. Bradley, A. J. Schoenwald, M. Wong, P. N. Mohammed, and J. R. Piepmeier, "Wideband digital signal processing test-bed for radiometric rfi mitigation," in *2015 IEEE International Geoscience and Remote Sensing Symposium (IGARSS)*, July 2015, pp. 3489–3492.

[3] E. Ollila, J. Eriksson, and V. Koivunen, "Complex elliptically symmetric random variables - generation, characterization, and circularity tests," *IEEE Transactions on Signal Processing*, vol. 59, no. 1, pp. 58–69, Jan 2011.

[4] S. Misra, P. N. Mohammed, B. Guner, C. S. Ruf, J. R. Piepmeier, and J. T. Johnson, "Microwave radiometer radio-frequency interference detection algorithms: A comparative study," *IEEE Transactions on Geoscience and Remote Sensing*, vol. 47, no. 11, pp. 3742–3754, Nov 2009.